Influence of the Base Element on the Thermal Properties of Non- Ferrous Chromium-Rich TaC-Containing Alloys Elaborated by Conventional Casting: Part 1: Thermodynamic Approach, Melting Ranges, as-Cast Microstructures and Thermal Expansion

Lionel Aranda, Patrice Berthod, Jean-Paul Gomis, Zohra Himeur

Influence of the Base Element on the Thermal Properties of Non-Ferrous Chromium-Rich TaC-Containing Alloys Elaborated by Conventional Casting: Part 1: Thermodynamic Approach, Melting Ranges, as-Cast Microstructures and Thermal Expansion

Lionel Aranda[1], Patrice Berthod[1,*], Jean-Paul K. Gomis[2] and Zohra Himeur[2]

[1]*Institut Jean Lamour (UMR 7198), University of Lorraine, Campus ARTEM, 2 allée André Guinier, BP 50840, 54000 Nancy, France*

[2]*Faculty of Science and Technologies, Campus Victor Grignard, Rue du Jardin Botanique, BP 70239 54500 Vandoeuvre-lès-Nancy, France*

Abstract: After preliminary thermodynamic calculations for verifying their refractoriness, six (Ni,Co)-based alloys were synthesized by casting. They contain chromium, carbon and tantalum to achieve interesting chemical and mechanical high temperature properties. Their microstructures in the as-cast state were observed by electron microscopy (SEM) to discover the carbides characteristics. Differential thermal analysis (DTA) was carried out for all of them to assess their melting points notably, for having better knowledge about the level of high temperature at which they can be used potentially. Thereafter thermomechanical analyses (TMA) were run to explore their behaviour in thermal expansion. As shown by the thermodynamic calculations all the alloys are theoretically possible to be shaped by conventional foundry due to liquidus temperatures all below 1400°C. According to these same results, the solidus temperatures of all alloys would stay over 1250°C, this suggesting that all alloys would be able to be used under moderate mechanical stresses at temperatures as high as 1200°C. As suggested by calculations, the as-cast microstructures are all dendritic and the interdendritic spaces are occupied by carbides. According to calculations again, the Ni-richest alloys contain chromium carbides, but tantalum carbides are also present, a presence which was not expected. In contrast the Co-richest versions contain only TaC carbides. The DTA experiments show that the solidus and liquidus temperatures both increase by going from the Ni-richest alloys to the Co-richest ones. The TMA experiments demonstrate that the thermal expansions and thermal contractions are rather continuous, without any irregularities, and the average thermal expansion coefficients, all close to $20 \times 10^{-6} K^{-1}$, do not systematically depend on the respective proportions of nickel and cobalt. This first part of the whole work will be followed by two other parts dealing with the effect of these Ni and Co proportions on the high temperature oxidation phenomena, for temperature variations and for isothermal conditions respectively.

Keywords: Cast alloys for high temperature, nickel and cobalt, tantalum carbides, thermodynamic calculations, thermal analysis, as-cast microstructure, thermodilatometry.

INTRODUCTION

Non-ferrous alloys based on nickel and/or cobalt elaborated by classical foundry are inexpensive alternative solutions to high performance but costly superalloys for some high temperature applications. This is the case of Fe-free equi-axed cast alloys based on nickel and cobalt containing chromium for {hot corrosion}-resistance purpose and tantalum carbides for good level of mechanical properties at high temperature. For the role of base element nickel can remain alone to form the dendritic structure which will contain a part the other elements (Cr, Ta, C) in solid solution. This is also true for cobalt. But it can be more interesting to mix these two elements to take benefit, in alloys based on Ni and Co together, of the advantages that each of them may bring, notably matrix stabilization in austenitic structure and good oxidation behavior for nickel [1], high mechanical strength at elevated temperature for cobalt [2].

Tantalum carbides are known to be very refractory and stable at elevated temperatures. They can be met in nickel-based superalloys [2], equi-axed [3-5] or directionally solidified [6], in which they can be in competition with other MC carbides (e.g. M=Nb). In cobalt-based alloys TaC features among the most met strengthening carbides [7-9]. In order to obtain strengthening efficient enough, the TaC quantity must be rated at values allowing good interdendritic cohesion without risking lack of toughness. The carbon content may be chosen around 0.5wt.% and, to favor TaC at the expense of other types of carbides, the corresponding weight content of Ta leading to the molar equivalence between C and Ta is to prefer. For 0.4wt.%C 6wt.%Ta must be thus chosen. This is with this base, and for a 25wt.% content in chromium, that the effect of the Ni-Co balance on the thermal properties which was studied. In the present first part

Address correspondence to this article at the Institut Jean Lamour (UMR 7198), University of Lorraine, Campus ARTEM, 2 allée André Guinier, BP 50840, 54000 Nancy, France; Tel: (+33) 3 72 74 27 29;
E-mail: patrice.berthod@univ-lorraine.fr

E-ISSN: 2410-4701/19

we will present some results of preliminary thermodynamic calculations to have first knowledge of the refractoriness which can be expected for alloys with these C, Ta and Cr contents for a Co (or Ni) content varying from 0 to the maximal possible content (68.6wt.% after the Cr, Ta and C contents deductions). In a second time the real alloys will be synthesized by conventional foundry and their as-cast microstructures examined. Thereafter the high temperature capabilities of these alloys will be explored by experimentally verifying their temperatures of fusion beginning. Finally the absence of any molten zone even very little will be checked by performing thermodilatometry test up to the highest temperature which was considered for possible uses with the knowledge of the fusion start temperatures previously measured.

MATERIALS AND METHODS

Thermodynamic Calculations

In a first time thermodynamic calculations were carried out to explore the high temperature equilibria of the {0 to 68.6 Co, 68.6 to 0 Ni, 25Cr, 0.4C, 6Ta (all contents in wt.%)} system, with special focus of the lowest limit of existence or co-existence of the liquid phase. This was done using the N version of the Thermo-Calc software [10], working with a database built on the base of the SSOL existing one [11] by S. Michon [12]. One can shortly remind that such calculations consist in identifying, for a given chemical composition and for given values of temperature and pressure, the combination of phases (liquid with the different possible solid phases) leading to the minimal free enthalpy for the alloy.

Choice and Synthesis of the Alloys for the Experimental Part of the Study

A cobalt-free Ni-based alloy (named “0Co5NiTa”) and a nickel-free Co-based alloy (named “5Co0NiTa”) were first considered. Four alloys were added to represent the whole range of alloys between the two former ones, with Co and Ni contents regularly distributed (from the “4Co1NiTa” alloy to the “1Co4NiTa” one). The wished chemical compositions of all alloys are displayed in Table **1**.

Pure elements (Alfa Aesar, purity > 99.9 wt.%) were taken and weighed in order to obtain 40g-charges to melt with the wished compositions. The used furnace was a high frequency induction one: CELES 50kW (operating parameters: internal atmosphere: 300mbars of pure argon, frequency: around 110kHz, voltage: 4kV, temperature level during the 5 minutes-liquid homogenization stage: about 1600°C, total duration from heating start and ingot cooled to room temperature: about 40 minutes).

Chemical Compositions Control and as-Cast Microstructures Examinations

After complete cooling, each of the six ingots was cut with metallographic saws to obtain the different samples for the different types of investigations. In this first part of the total work three pieces of ingot were obtained. One of them was embedded in a cold resin mixture (ESCIL), ground and polished. The mirror-like metallographic sample was observed with a SEM (Scanning Electrons Microscope: JEOL, JSM-6010LA) in BSE (Back Scattered Electrons) mode. The chemical compositions were controlled using the EDS (Energy Dispersion Spectrometer) attached to the SEM.

Temperature Melting Ranges

A second piece of each ingot was devoted to DTA (Differential Thermal Analysis). The approximate dimensions of the sample were 2 × 2 × 7 mm^3. Placed in a little alumina crucible it was subjected to a thermal cycle composed of a fast heating up to 1000°C (+20°C/min), a slow heating from 1000 to about 1450°C (+5°C/min) a slow cooling from 1450 to 1000°C (-5°C/min) and a fast cooling down to ambient temperature (-20°C/min). The heat flow exchanged between the studied sample and the machine allowed

Table 1: The Names and the Wished Chemical Compositions of the Alloys for the Study

0Co5NiTa	1Co4NiTa	2Co3NiTa	3Co2NiTa	4Co1NiTa	5Co0NiTa
0 wt.%Co	14 wt.%Co	27 wt.%Co	Base Co	Base Co	Base Co
Base Ni	Base Ni	Base Ni	27 wt.%Ni	14 wt.% Ni	0 wt.% Ni
25 wt.%Cr	25 wt.%Cr	25 wt.%Cr	25 wt.%Cr	25 wt.%Cr	25 wt.%Cr
0.4 wt.%C	0.4 wt.%C	0.4 wt.%C	0.4 wt.%C	0.4 wt.%C	0.4 wt.%C
6 wt.%Ta	6 wt.%Ta	6 wt.%Ta	6 wt.%Ta	6 wt.%Ta	6 wt.%Ta

detecting the starts and ends of melting and of solidification.

Thermal Expansion and High Temperature Dimensional Stability

To complete the DTA data, thermodilatometry runs were also performed for a third piece par ingot. A small parallelepiped with approximate dimensions 4 × 4 × 2.5 mm^3 was placed between the alumina pieces of the thermodilatometer (SETARAM 96Line Evo). A thermal cycle composed of a 10°C/min heating up to 1250°C, a 1hour-isothermal stage at 1250°C and a -10°C/min-cooling down to ambient temperature was applied. The heating part was considered for checking that no melting occurred and also for specifying thermal expansion coefficients. The purpose of the isothermal stage was to observe whether a compressive visco-plastic deformation took place, to also verify the absence of any liquid at this temperature.

RESULTS AND DISCUSSION

Thermodynamic Calculations

The preliminary thermodynamic calculations led to the isopleth section of the quinary diagram, presented in Figure **1**. This suggests that each alloy should be still solid up to 1250°C. However the solidus temperatures of the 1Co4NiTa, 2Co3NiTa, 3Co2NiTa and 4Co1NiTa alloys remain close to these 1250°C while the two quaternary alloys, 0Co5NiTa and 5Co0NiTa, are at least 50°C more refractory. The mushy zone (Liquid + Matrix) extends up to 1400°C maximum, which indicates that no problem of not total melting can be feared for the real elaborations.

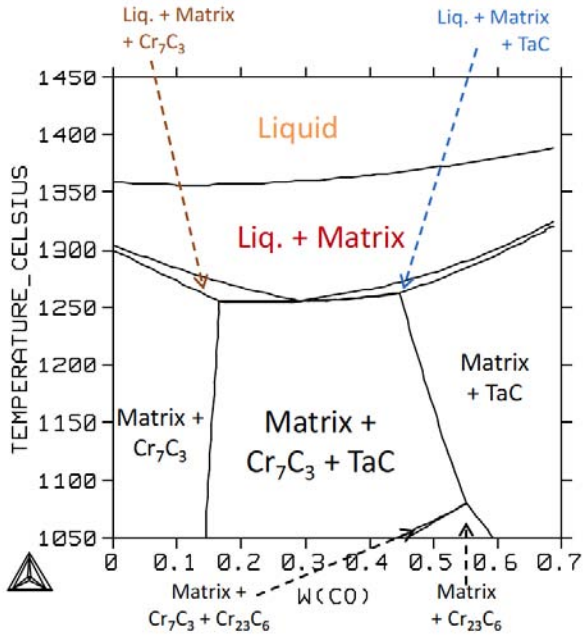

Figure 1: The isopleth section of the {Ni, Co, Cr, Ta, C} diagram for 25wt.%Cr, 0.4wt.%C and 6wt.%Ta (Co increasing from 0 to 68.6wt.% at the expense of Ni).

After thermodynamic calculations other information is also available. One can notice that the presence of a double-phased {liquid + matrix} zone separating the totally liquid and the totally solid areas suggests that solidification should start with the crystallization of dendrites of matrix (which is Face Centred Cubic for all alloys over the temperature range concerned by Figure **1**). At lower temperature, either high temperature chromium carbides (Cr_7C_3) or tantalum monocarbides (TaC) for Ni-rich and Co-rich alloys respectively, should precipitate from the residual liquid, as is to say in the interdendritic spaces. The Co-free Ni-based alloy should finish its solidification in a double-phased microstructural state (FCC matrix + Cr_7C_3). This is the same for the Ni-free Co-based alloy but with TaC instead Cr_7C_3. Concerning the four intermediate alloy it can be expected that the precipitation of Cr_7C_3 will be followed by the precipitation of TaC or inversely, for a final triple-phased microstructure composed of FCC matrix dendrites and Cr_7C_3 and TaC interdendritic carbides. Taking into account the rather fast solid state cooling one can think that the microstructures which will be finally obtained for the real alloys will be not very different from what they were just after solidification.

As-Cast Microstructures of the Real Alloys

The elaboration of each of the six alloys was achieved without encountering any problem. Seemingly the melting was total, with no not-melted parts visible in the periphery of the ingots or in the sections observable after the sawing operations. After the metallographic preparation described above the microstructures were observed with the SEM in BSE mode. Some micrographs illustrate the microstructures in Figure **2** for the two Ni-richest alloys, Figure **3** for the two intermediate alloys (neither Ni nor Co is predominant) and in Figure **4** for the two Co-richest alloys. In each figure the micrographs presented on the left are general view (low magnification: × 250) and the ones presented on the right are detailed view (higher magnification: × 1000). With the low magnification micrograph one can see that the as-cast microstructures of all alloys are effectively dendritic and that the carbides are located in the interdendritic spaces, this indicating that they effectively appeared at the end of solidification. This is true for the chromium

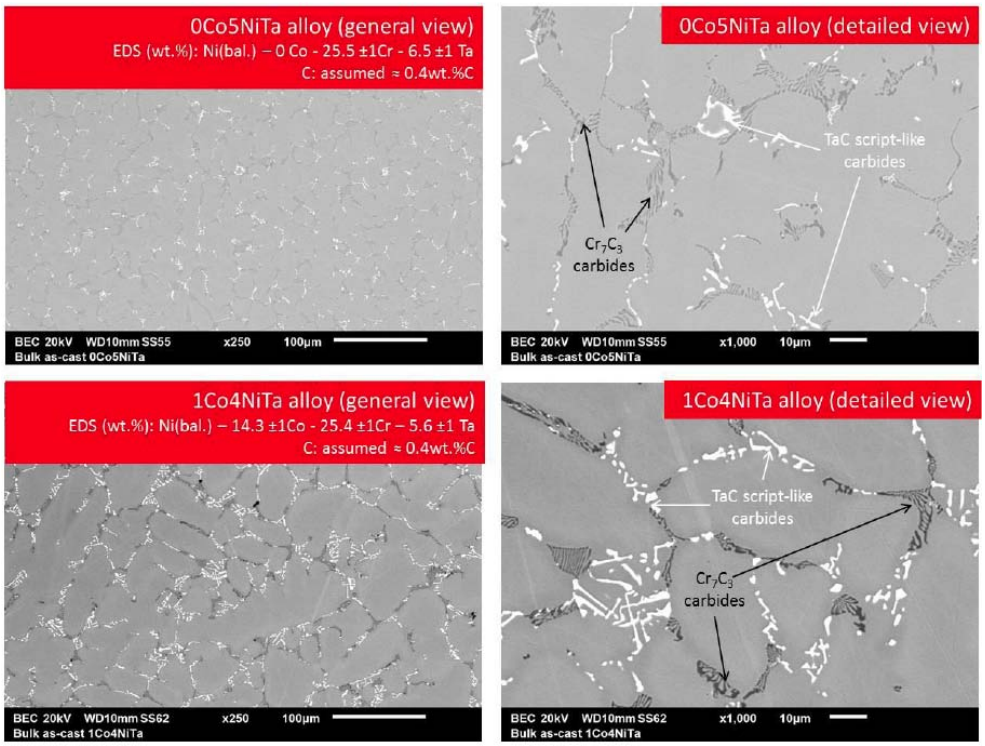

Figure 2: Microstructures of the two nickel-richest alloys in their as-cast states (top: 0Co5NiTa, bottom: 1Co4NiTa, left: ×250, right: ×1000); left: composition measured by 5 full frame EDS on ×250 areas.

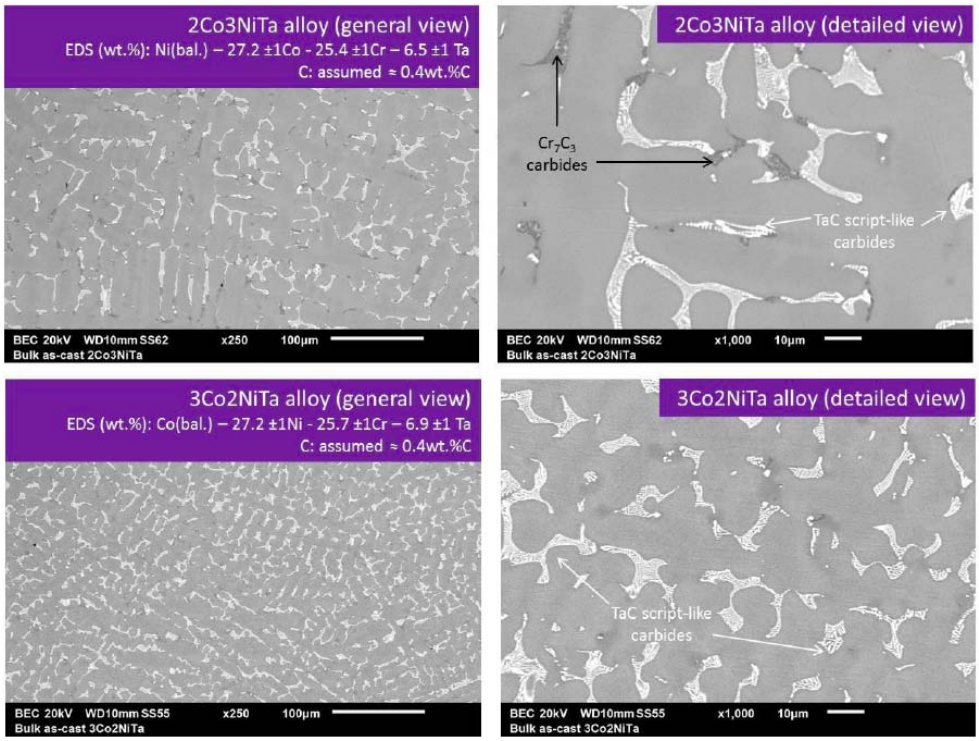

Figure 3: Microstructures of the two intermediate alloys in their as-cast states (top: 2Co3NiTa, bottom: 3Co2NiTa, left: ×250, right: ×1000); left: composition measured by 5 full frame EDS on ×250 areas.

carbides (darker than matrix) as well as for the tantalum carbides (brighter than matrix), natures confirmed by spot EDS analysis.

DTA Results and Melting Ranges

The results coming from the differential thermal analyses which were carried out for each of the six

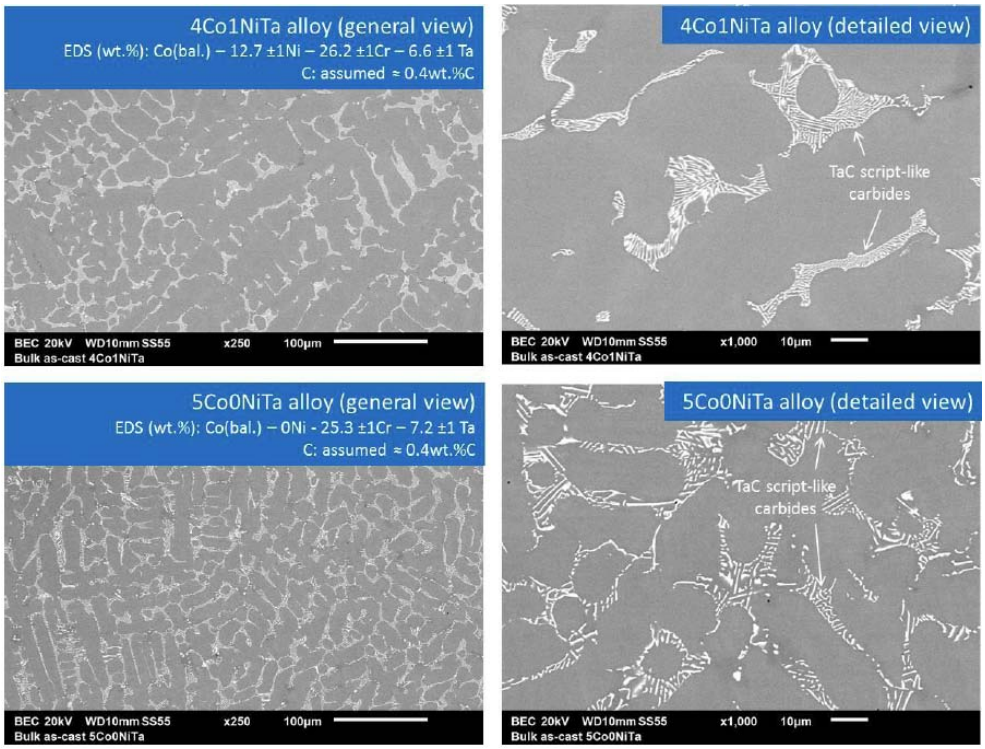

Figure 4: Microstructures of the two cobalt-richest alloys in their as-cast states (top: 4Co1NiTa, bottom: 5Co0NiTa, left: ×250, right: ×1000); left: composition measured by 5 full frame EDS on ×250 areas.

alloys are presented in Figure **5** for the two Ni-richest alloys, Figure **6** for the two intermediate alloys and in Figure **7** for the two Co-richest alloys. Each curve is composed of a first half corresponding to heating (enhanced in its high temperature part which is the zone of interest) and a second part (cooling, high temperature only). In the heating part of the curves one notices two or three peaks linked to two or three endothermic transformations (melting of one or of two successive eutectic compounds, followed by the melting of the remaining matrix). Similarly, the cooling part owns two or three exothermic peaks (crystallization of a part of the matrix, followed by the successive eutectic solidifications of the two types of eutectic compounds). As usually observed for heating and cooling applied with not very low rates, the melting start temperatures of the different phases or compounds are delayed then shifted to slightly higher

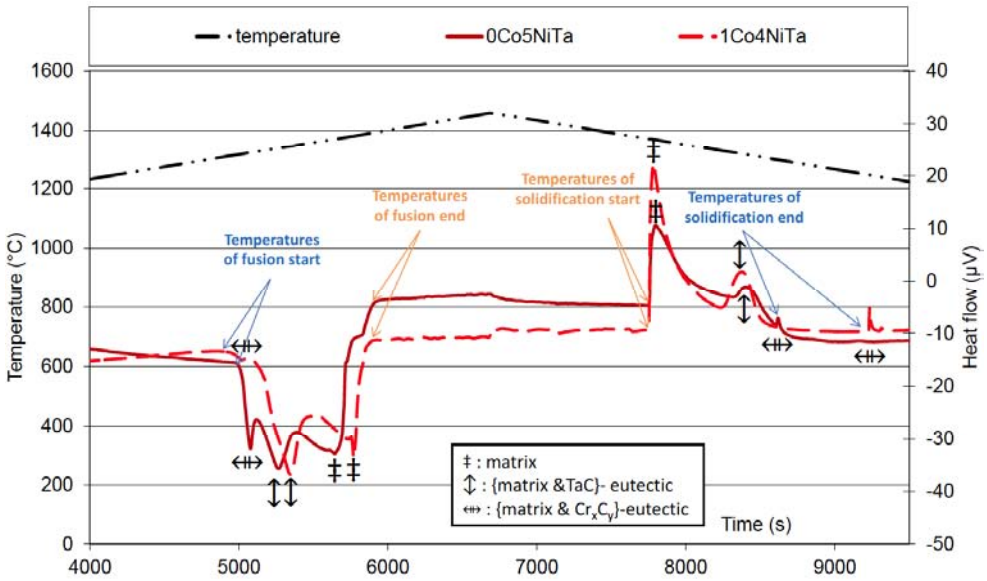

Figure 5: The DTA curves obtained for the two richest-richest alloys.

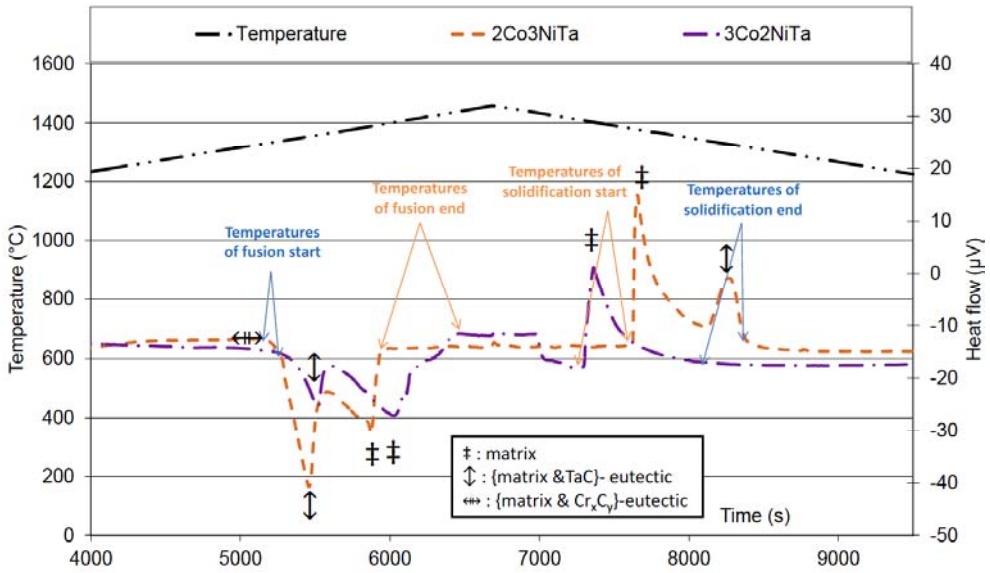

Figure 6: The DTA curves obtained for the two intermediate alloys.

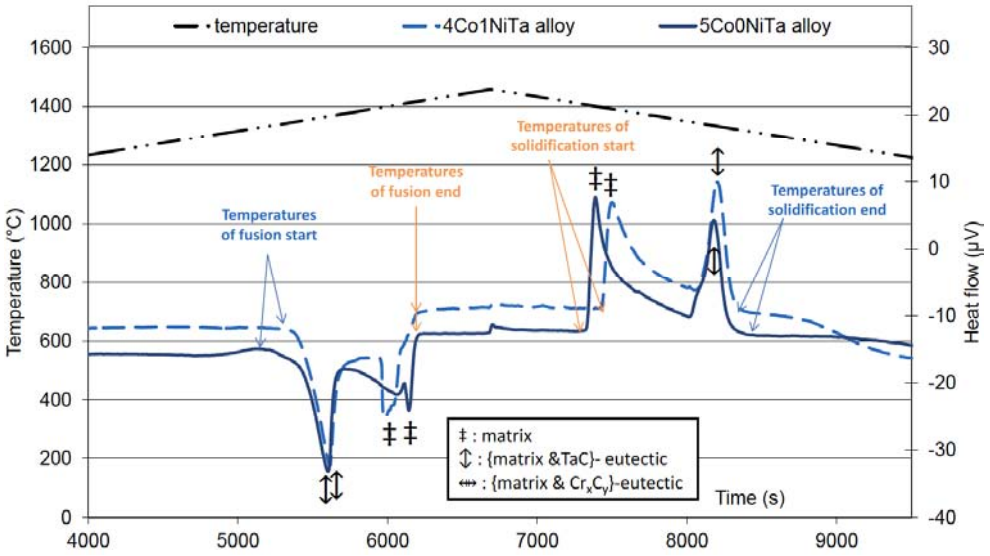

Figure 7: The DTA curves obtained for the two cobalt-richest alloys.

temperatures while the solidification start temperatures are shifted to lower temperatures, especially the temperature of crystallisation start of the first solid phase to appear (late because delayed nucleation, and low temperature because rather great overcooling) which is marked by a particularly sudden heat emission. The DTA curve corresponding to the Co-free Ni-based alloy (0Co5NiTa) logically contains three endothermic peaks and three exothermic peaks, taking into account the presence of two distinct eutectic compounds and one phase. Curiously this is not the case for the 1Co4NiTa alloys the microstructure of which looked like the one of the former alloy. In contrast, the presence of two endothermic (respectively exothermic) peaks in the heating part (resp. cooling) of the DTA curves of the four other alloys is in good accordance with the very small presence of chromium carbides or their total absence.

The temperatures of melting start and of melting end as well as the corresponding temperatures for solidification were noted and their values are plotted versus the chemical composition of the alloys in Figure **8**.

Plotting these results together allows a clear observance that the start and end of transformations are shifted toward higher temperatures at heating and lower temperatures at cooling. Despite these hysteresis-type phenomena, one can see that the

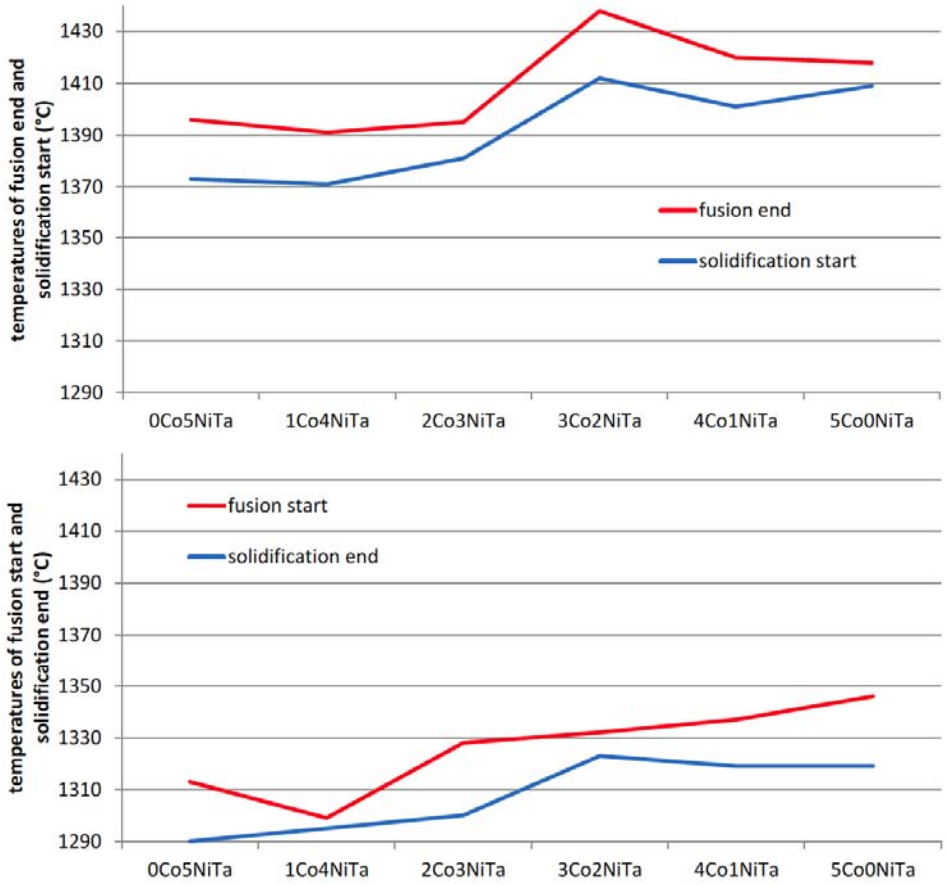

Figure 8: The temperatures of fusion end and solidification start (top) and the values of fusion start and solidification end (bottom).

melting start and solidification end temperatures globally increase regularly when there is more and more cobalt and less and less nickel in the alloy. The same global tendency seems to exist for the melting and solidification start temperatures (except for the 3Co2NiTa for which a curious result was obtained). However there is a slight decrease in these temperatures between the 0Co5NiTa alloy and the 1Co4NiTa one, but this is qualitatively in good agreement with the preliminary thermodynamic calculations (Figure **1**). This good qualitative agreement between calculations and experiments is also true for the evolution versus the Co content for the following alloys. Quantitatively, discrepancies are obvious between theory and reality: the liquidus temperatures issued from calculations are significantly lower than the measured ones. This is the same the calculated solidus temperatures and the measured ones.

Thermodilatometry Results

Thermal expansion of the six alloys was characterized by dilatometry. Two examples are given in Figure **9** (case of the nickel-rich 1Co4NiTa alloy) and in Figure **10** (case of the cobalt-rich 4Co1NiTa alloy). All curves heating and cooling are similar to one another, with a regular expansion slightly accelerating when temperature increases, without any discontinuity, even for alloys for which possible allotropic change of matrix can be expected (the cobalt-richest alloys). The final total expansion may be more or less different among the six alloys but these differences are rather small. The cooling curves show a continuous contraction decelerating when temperature decreases, here too without any irregularity for instance caused by allotropic transformation. The final residual deformation may be inexistent (e.g. 1Co4NiTa, Figure **9**-left) or slightly positive (e.g. 4Co1NiTa, Figure **10**-left) or slightly negative. Even if no residual deformation remains after return to room temperature the heating part and the cooling part are generally not superposed but they form a kind of hysteresis. During the hour spent at 1250°C a little deformation no real deformation occurred (e.g. 4Co1NiTa, Figure **10**-right) or not (e.g. 1Co4NiTa, Figure **9**-right). But, when existing, these isothermal deformations are very small and cannot really be correlated with the residual deformation

observed after return to room temperature in some cases. No start of melting was detected since in such case this is sure that the deformation should decelerate before arriving to 1250°C and continue during the 1 hour – isothermal exposure before cooling.

One can compare these results with the ones obtained earlier for similar alloys. On pure metals M, binary M30Cr and ternary M30Cr0.8C (wt.%; M=Ni, Co or Fe) heated up to 1200°C and maintained 2 hours at this temperature before cooling, the dimensional changes were more sometimes more perturbed with the allotropic transformation evidencing of Co, Fe and Co-30Cr (hcp → fcc and bcc → fcc) and the compressive effect of the chromium carbides on the matrix close to 1200°C [13]. Similar phenomena were observed for Fe-30Cr and (Fe=Ni)-30Cr containing high fractions of TaC carbides [14], as well as for Ni-30Cr-1C and Co-10Ni-30Cr-0.5C-7.5Ta alloys except when their chromium carbides or tantalum carbides were preliminarily fragmented by a long high temperature exposure. The phenomena observed for these alloys earlier studied did not occur for the present alloys. This is probably due to the Cr lower content and to carbides population a little less dense than the ones in the alloys earlier studied. Indeed, chromium is known to accelerate thermal expansion in some cases. This was observed notably for nickel and cobalt-based alloys (e.g. [13]). Second, in case of the presence of an interdendritic carbide network dense enough to be interconnected, the difference in thermal expansion between the matrix (typical average thermal expansion coefficient: 20×10^{-6} K^{-1}) and carbides (less than half this value), a progressive compressed state of the matrix under the action of the carbides and elongated state of the carbides under the action of the matrix finish to induce a visco-plastic compressive deformation of the matrix under the action of the carbides as soon as temperature is high enough to weaken the matrix [13-15]. If the dense network became preliminarily fragmented during a high temperature exposure applied before the dilatometry test this phenomenon can be attenuated and even annulled [15]. One can think that the same result may be obtained when the carbon content and/or carbide former-metal content are chosen at lower values to decrease the carbides network density and suppress its interconnection, which can be achieved even by chosen 0.4C-6Ta against 0.5C-7.5Ta.

To finish with the dilatometry results some characteristics were measured or noted on all the obtained curves and studied versus the Co-enrichment at the expense of nickel, from the 0Co5NiTa alloy to the 5Co0NiTa alloy. The average thermal coefficient specified on the heating part and the one specified on the cooling part of the dilatometry curves are plotted in Figure **9** while the deformation achieved during the whole heating, the deformation existing at the end of the isothermal stage, and the residual deformation after return to room temperature, are plotted in Figure **10**. At heating the thermal expansion coefficient seems to be minimal for the intermediate alloys (with Ni and Co contents not too far from one another) but this is not really found again at cooling. Concerning the deformation at the end of heating, it logically follows the same trend as the average thermal coefficient. For the residual deformation at the return to room temperature it seems that positive residual deformation remains for the Ni-richest or Co-richest alloys and minimal, inexistent and even negative for the intermediate alloys.

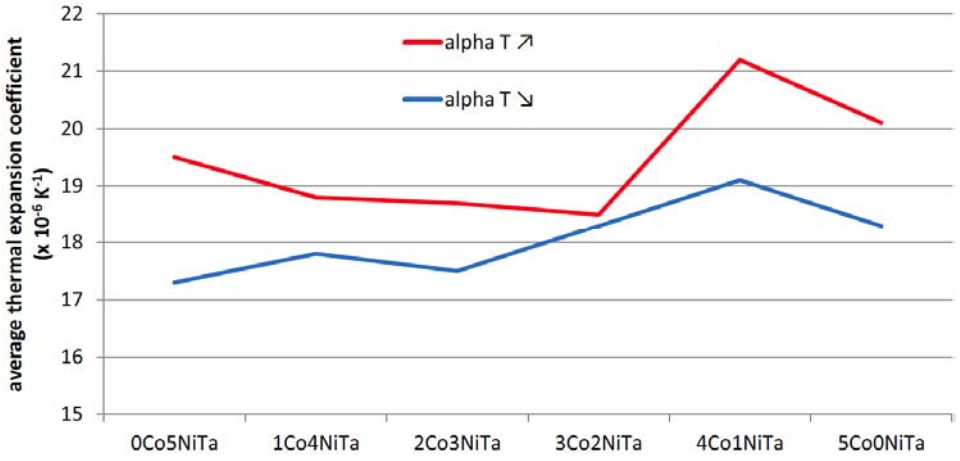

Figure 9: Variation, versus the Co enrichment at the expense of Ni, of the average thermal coefficient specified on the heating part and the one specified on the cooling part of the dilatometry curves.

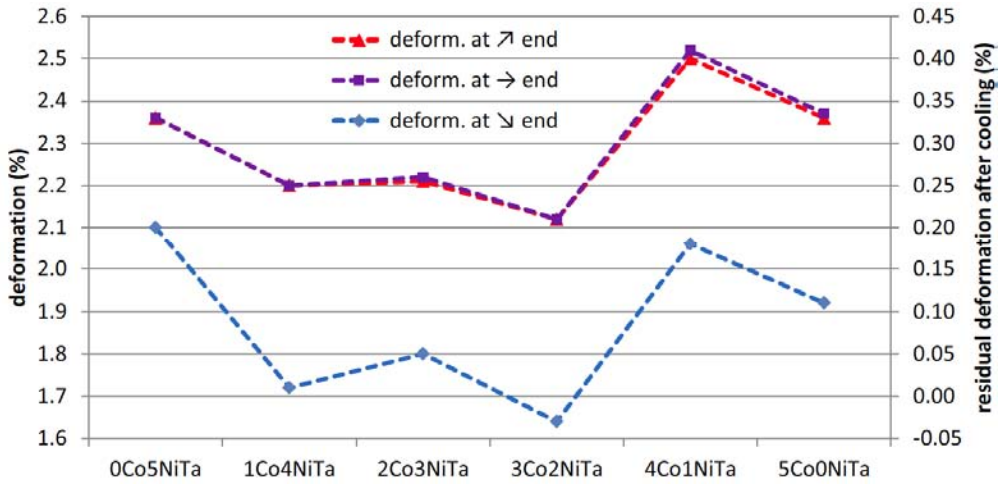

Figure 10: Variation, versus the Co enrichment at the expense of Ni, of the deformation achieved during the whole heating, of the deformation existing at the end of the isothermal stage and the residual deformation after return to room temperature.

An interesting information is the slight but visible decrease in thermal expansion coefficient here observed for the intermediate alloys by mixing Ni and Co at the base element position rather than considering the Co-free Ni-based alloy or the Ni-free Co-based alloy. Indeed lowering thermal expansion is often of great interest for alloys working in conditions of varying temperatures, to limit the induced internal stresses. Unfortunately no evident explanation of this interesting effect of mixing Ni and Co as base element can be currently provided. Especially devoted investigations on alloys with the same chemical compositions and microstructures, but with controlled microstructural orientation (e.g. directionally solidified, not equi-axed as here) must be carried out to confirm and interpret this observation.

CONCLUSIONS

The nature of the base element, the one present with the highest weight content in the alloy, was logically expected to have high impact on the properties and the behavior of the alloy, for given contents in all the other elements present in the chemical composition. Noticeable effect was seen here on the carbides natures in the as-cast state of the alloys (Ni authorizing the presence of chromium carbides beside the tantalum carbides, Co favorable to the exclusive presence of the TaC), the refractoriness (favored by Co) and melting range, and also, but with more in moderation, the thermal expansion of the whole alloy. In the two following parts of this work, these are the effects of the overall behavior in oxidation at high temperature which will be investigated, first the starts of oxidation at heating and the oxide spallation at cooling [16] and second the isothermal surface and sub-surface degradation of the alloys during isothermal oxidation at high temperature.

REFERENCES

[1] Young DJ. High Temperature Oxidation and Corrosion of Metals, Elsevier, Amsterdam 2008.

[2] Donachie MJ, Dionachie SJ. Superalloys: A Technical Guide (2nd edition), ASM International, Materials Park 2002.

[3] Youdelis WV, Kwon O. Metal Science 1983; 17(8): 385. https://doi.org/10.1179/030634583790420673

[4] Janowski GM, Heckel RW, Pletka BJ. Metallurgical Transactions A: Physical Metallurgy and Materials Science 1986; 17A(11): 1891. https://doi.org/10.1007/BF02644987

[5] Zheng L, Zhang G, Lee TL, Gorley MJ, Wang Y, Xiao C, Li Z. Materials & Design 2014; 61: 61. https://doi.org/10.1016/j.matdes.2014.04.055

[6] Zhang W, Liu L, Fu H. China Foundry 2012; 9(1): 11.

[7] Youdelis WV, Kwon O. Metal Science 1983; 17(8): 379. https://doi.org/10.1179/030634583790420664

[8] Gui W, Zhang H, Yang M, Jin T, Sun X, Zheng Q. Journal of Alloys and Compounds 2017; 728: 145. https://doi.org/10.1016/j.jallcom.2017.08.287

[9] Gui W, Zhang X, Zhang H, Sun X, Zheng Q. Journal of Alloys and Compounds 2019; 787: 152. https://doi.org/10.1016/j.jallcom.2019.02.041

[10] Thermo-Calc Version N. Foundation for Computational Thermodynamics, Stockholm, Sweden, Copyright, 1993, 2000. www.thermocalc.com

[11] SSOL Database, SGTE Solutions Database, Scientific Group Thermodata Europe, Bo Sundman, Stockholm, Sweden, 1992.

[12] Michon S. PhD thesis, University Henri Poincaré Nancy I, 2004.

[13] Berthod P. International Journal of Materials Research (formerly Z. Metallkd) 2008; 99(3): 265.

[14] Berthod P, Aranda L, Hamini Y. Materials Science 2011; 47(3): 319. https://doi.org/10.1007/s11003-011-9399-0

[15] Berthod P, Heil C, Aranda L. Journal of Alloys and Compounds 2010; 504: 243. https://doi.org/10.1016/j.jallcom.2010.05.101

[16] Berthod P, Aranda L, Medjahdi G, Gomis J-PK. Journal of Materials Science and Technology Research 2019; 6: 63-72. https://doi.org/10.15377/2410-4701.2019.06.8

[17] Gomis J-PK, Berthod P, Etienne E. Journal of Materials Science and Technology Research 2019; 6: 73-83. https://doi.org/10.15377/2410-4701.2019.06.9

Received on 30-09-2019 Accepted on 17-10-2019 Published on 25-10-2019

DOI: https://doi.org/10.15377/2410-4701.2019.06.7